Self-Healing Actuating Adhesive Based on Polyelectrolyte Multilayers

*Yuanqing Gu and Nicole S. Zacharia**

Creating actuators capable of mechanical motion in response to external stimuli is a key for design and preparation of smart materials. The lifetime of such materials is limited by their eventual wear. Here, self-healable and adhesive actuating materials are demonstrated by taking advantage of the solvent responsive of weak polyelectrolyte multilayers consisting of branched poly(ethylenimine)/poly(acrylic acid) (BPEI/PAA). BPEI/PAA multilayers are dehydrated and contract upon contact with organic solvent and become sticky when wetted with water. By constructing an asymmetric heterostructure consisting of a responsive BPEI/PAA multilayer block and a nonresponsive component through either layer-by-layer assembly or the paste-to-curl process, smart films that actuate upon exposure to alcohol are realized. The curl degree, defined as degrees from horizontal that the actuated material reaches, can be as high as ≈228.9°. With evaporation of the ethanol, the curled film returns to its initial state, and water triggers fast self-healing extends the actuator's lifetime. Meanwhile, the adhesive nature of the wet material allows it to be attached to various substrates for possible combination with hydrophobic functional surfaces and/or applications in biological environments. This self-healable adhesive for controlled fast actuation represents a considerable advance in polyelectrolyte multilayers for design and fabrication of robust smart advanced materials.

1. Introduction

Actuating materials, which are able to turn an external stimulus into a dimensional change or motion, have been intensely studied in order to provide components for advanced devices such as artificial muscles, cantilever sensors, automated switches, and microrobots.[1] Polymers have attracted particular interest as smart actuator materials, as their structural variety enables unique responses under a range of specific external stimuli.[2] For example, the thermal transition of poly(*N*-isopropylacrylamide) based hydrogels based on their low critical solution temperature causes a rapid deswelling and bending upon heating,[3,4] block copolymers with both hydrophobic and hydrophilic blocks present humidity dependent swelling behaviors,[5] electroconductive conjugated polymers demonstrate electric field responsive actuation,[6] and the dehydration of polyelectrolytes (PEs) in layer-by-layer (LbL) assemblies upon exposure to organic vapor results in a rapid dimensional change that can be used for actuation.[7] Durability of polymeric actuating devices remains an issue, especially for ionic actuators due to failure of the various components of the device.[8] Another limitation when fabricating these devices other adhesives or other strategies are required to affix the actuating material to other surfaces (e.g., metal electrodes, hydrophobic plastics, or biological cell surfaces) in order to incorporate them into devices, which may inhibit actuation behavior. Presented here is a simple and effective approach to overcome these obstacles using a wet adhesive, self-healing actuating material that may prove useful in applications such as sensors, smart lifts, and automatic gates.

It has recently been demonstrated that the sticky and flowable nature of adhesive materials can be used for self-healing.[9] In one instance a prolonged control over strain and under electric field has been observed for self-healable composites consisting of dielectric elastomers and silicone.[10,11] While these composites require an external electric field and just available for strain change, flowable polyelectrolytes in layer-by-layer assembled polyelectrolyte multilayers (PEMs) can achieve intrinsic self-healing of surface defects by simply being wet with water,[12–16] a large simplification over other approaches such as the inclusion of embedded healing agents.[17–22] Weak polyelectrolyte complexes become viscous upon contact with water,[23] and even show strong adhesive property if sufficiently concentrated.[24] Such facile self-healing behavior can be used to extend the lifetime of actuating materials.

One of the most attractive features of electrostatically bound PEMs prepared by the LbL process is the controllable charge density of the PE chains, which can be adjusted by either controlling ionic strength of the surrounding aqueous solution for strong PEs or changing the ionic strength as well as solution pH for weak PEs with labile functional groups (e.g., carboxylic acid).[24] This ability to modulate polyelectrolyte charge density will in turn tune the properties of the PEMs, creating changes in thickness, swelling/shrinking states, elastic properties, porosity, wettability, and even generates determined mechanical motions.[23,25,26] This makes PEMs, especially those made from

Dr. Y. Gu, Prof. N. S. Zacharia
Department of Polymer Engineering
University of Akron
Akron, OH 44325, USA
E-mail: nzacharia@uakron.edu

DOI: 10.1002/adfm.201501055

weak polyelectrolytes, ideal for responsive materials,[27] such as pH,[28] electric field,[29] and electrochemically induced swelling in water,[30] thermoresponsive film expansion,[31] and humidity controlled curling behavior[32] as well as "walking."[33] However, for these diverse reversible actuators, thin PEMs are preferable to achieve significant dynamic motion,[34] which limits the adhesive force as well as PE migration rate needed for effective self-healing performance when the PEs are ionically bound to the underlying substrate.[12,13]

Here, a free-standing adhesive capable of self-healing and significant actuation is created with LbL assembly and then by adhering this weak polyelectrolyte based material (specifically made from branched poly(ethylene imine)/poly(acylic acid) or BPEI/PAA) onto one side of a nonshrinking, flexible substrate. The PEM exhibits a significant contraction upon exposure to ethanol meaning that the asymmetric structure as a whole will curl in response to this stimulus and then return to flat with the evaporation of the ethanol and rehydration of the PEM. The film curl degree, as defined by degrees from horizontal reached by the actuating material,[23] is readily controlled by the percentage of ethanol in the solution used to generate the actuation and the mechanical properties of the nonresponsive portion of the bilayer structure. By facile treatment with deionized (DI) water, the film is able to restore itself from physical damage and to regain its mechanical properties, extending the number of actuation cycles possible. The film wet with water is also viscous allowing it to be adhered to various substrates regardless of their surface properties.

2. Results and Discussion

In situ spectroscopic ellipsometric analysis shows that the thickness of a film consisting of 50 poly(diallyldimethylammonium chrloride)/polystyrenesulfonate bilayers (denoted as $(PDAC/SPS)_{50}$ hereafter) swells to ≈117.27% of the initial dry thickness in a 50 vol% ethanol aqueous solution (**Figure 1**a). The swollen film thickness drops by exposing it to higher ethanol concentrations, and in pure ethanol it has essentially the same thickness as the dry film. However, for BPEI/PAA multilayers, the film thicknesses in ethanol–water solutions are even lower than the original dry thickness. Further analysis has confirmed that this is not due to a dissolution of the BPEI/PAA film.[23] Thus, BPEI/PAA multilayers will shrink as much as ≈9.62% by exposure to pure ethanol. This response is due to a dehydration of the PEM, enhancing interactions between polymer backbones therefore causing the film to contract.[23]

An actuator based on a heterostructured PEM system was prepared by successive LbL assembly of 50 BPEI/PAA bilayers and 50 PDAC/SPS bilayers onto a polystyrene substrate (**Scheme 1**). The hydrophilic free-standing $(BPEI/PAA)_{50}/(PDAC/SPS)_{50}$ film is readily removed from the hydrophobic polystyrene substrate due to the weak interaction between the two interfaces.[23] The surface roughness (*Ra*) obtained by stylus profilometry is 0.05 µm. A microscope image of the surface can be seen in the inset of **Figure 2**a and an atomic force microscope (AFM) image of the surface can be seen in Figure S1, Supporting Information. The average film thickness by profilometry (28.82 ± 0.11 µm) agrees with the sum of $(BPEI/PAA)_{50}$ (28.53 ± 0.13 µm) and $(PDAC/SPS)_{50}$ (176.1 ± 11.5 nm), with the weak PEs assembling loosely

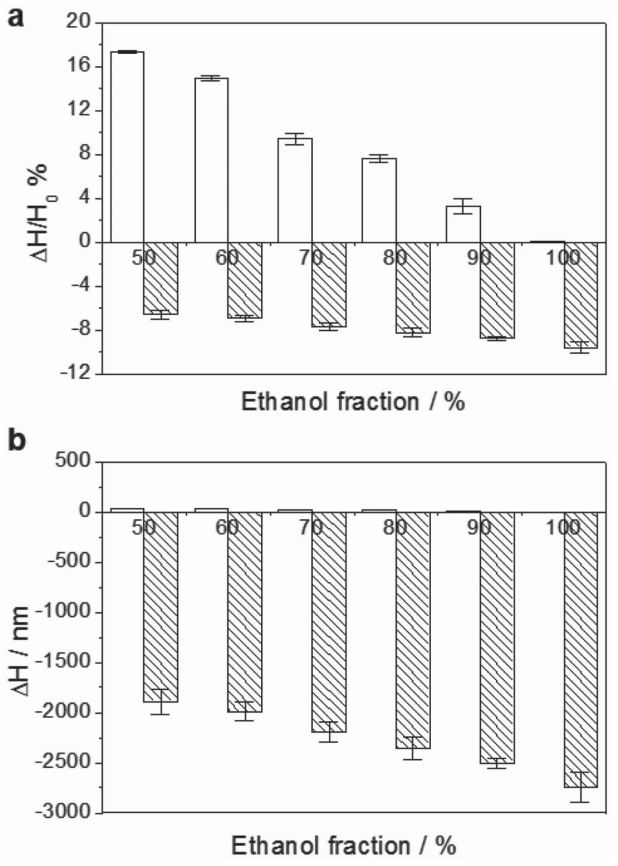

Figure 1. a) Film thickness change ratio of PDAC/SPS film (white bar) and BPEI/PAA film (shadowed bar) deposited on silicon wafers in different ethanol fraction solutions. b) Calculated film thickness change of $(PDAC/SPS)_{50}$ film and $(BPEI/PAA)_{50}$ film in different ethanol fraction.

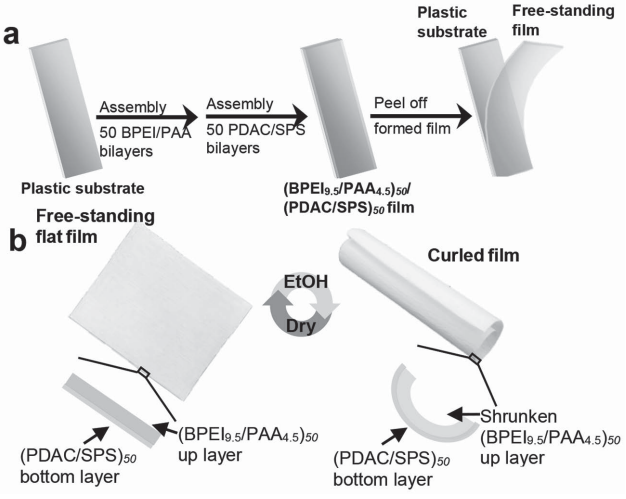

Scheme 1. Schematic illustrations of the fabrication process of the a) free-standing PEM film and b) repeatable switches between flat and curl states.

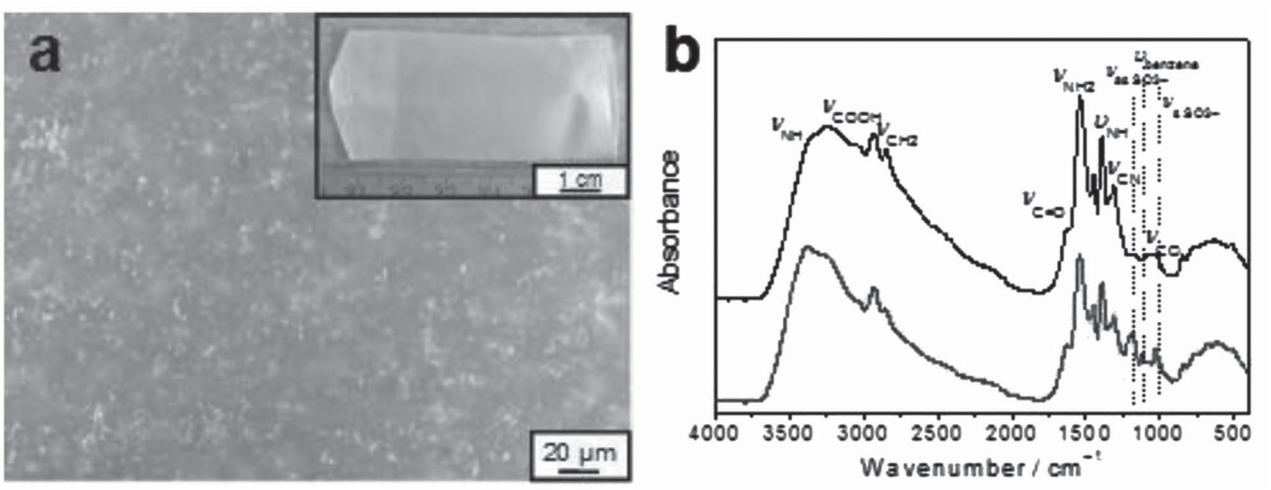

Figure 2. The as-prepared $(BPEI/PAA)_{50}/(PDAC/SPS)_{50}$ film. a) Microscope image of the film surface. The inset shows the film deposited on a plastic substrate. b) ATR-FTIR spectra of the BPEI/PAA side (top line) and PDAC/SPS side (bottom line) of the film.

and forming much thicker layers than the strong PEs.[35] The composition difference of the two film sides can be confirmed with attenuated total reflectance Fourier transform infrared (ATR-FTIR) spectroscopy which has a penetration depth below 5 μm.[36] Taking the spectra with the BPEI/PAA side pressed against the ATR crystal results in a spectrum identical to that normally observed for this system.[37,38] The spectrum from placing the PDAC/SPS against the crystal shows the in-plane skeleton vibration of the benzene ring (1130 cm^{-1}), the antisymmetric and the symmetric vibrational absorption bands of sulfonate group (1184 cm^{-1}, 1040 cm^{-1})[39] (Figure 2b). Moreover, $(BPEI/PAA)_{50}$ film consisting of only BPEI and PAA remains colorless transparent while a single side of the $(BPEI/PAA)_{50}/(PDAC/SPS)_{50}$ film turns blue after staining with 0.1 mg mL^{-1} methylene blue (MB) ethanolic solution for 10 min (Figure S2, Supporting Information). Though BPEI/PAA assembles loosely for the first eight bilayers, it becomes denser afterwards.[40,41] Meanwhile, the continuous LbL process avoids possible PEs permeation into the film upon swelling from the dry state. Therefore, the PDAC/SPS layer is uniformly deposited on a single side of the current film as an asymmetric heterostructured bilayer without diffusion of either block of the heterostructure into the other block.

The free-standing PEM heterostructure does not curl when exposed to pure DI water, 50 or 60 vol% ethanol treatment, but it does start to bend due to the uneven responses of the two blocks when 70 vol% ethanol is applied (Figure S3, Supporting Information). The curl degree, defined from the angle of curled film edges (Scheme S1, Supporting Information),[23,42] is proportional to the ethanol content in the solution applied to the film. In pure ethanol, the film curls immediately to $\gg 228.9°$ within 2 s (see Video S1, Supporting Information), while the free-standing $(BPEI/PAA)_{50}$ film does not curl under the identical ethanol treatment. This ethanol driven curl performance is far faster and more significant than the recently reported porous PEs membrane in the same size scale (2 mm × 4 mm × 40 μm, calculated curl rate ≤ 0.68 degree s^{-1}),[7] humidity responsive PEMs (equilibrate in 50–100 s)[32] as well as cross-linked PEMs (takes at least 6 s for bending ≈90°),[33] and ion sensitive hydrogels (bend for ≈90° over 1 h).[34] This rapid actuation originates from the BPEI/PAA layer, which shrinks significantly (≈2 μm, Figure 1b) and causes the entire structure to bend. The ethanol exposed film always bends along the shorter edge of the film while the longer edges curl up (Scheme S1b, Supporting Information), as the lower stress of the shorter edge facilitates the curling.

One commonly noted advantage of the LbL technique is that additional bilayer deposition (in linearly growing systems) can be used to create a thicker film without changing the film's chemical properties.[43] While the chemical composition of the $(BPEI/PAA)_{50}/(PDAC/SPS)_n$ films remains the same (Figure S4, Supporting Information), the curl degree upon exposure to pure ethanol respectively drops to ≈116.5°, ≈72.5°, and ≈17.5° for $(BPEI/PAA)_{50}/(PDAC/SPS)_{100}$, $(BPEI/PAA)_{50}/(PDAC/SPS)_{150}$, and $(BPEI/PAA)_{50}/(PDAC/SPS)_{200}$ films. Though the curl behavior is still to a much higher degree and faster than previously reported PEM based actuators,[7,32] it is clear that greater resistance from a thicker PDAC/SPS portion of the heterostructure inhibits the curl behavior (**Figure 3**).

Video S1, Supporting Information, shows that a $(BPEI/PAA)_{50}$ film remains flat after ethanol treatment, while a $(BPEI/PAA)_{50}/(PDAC/SPS)_{50}$ film curls when exposed to ethanol, and it gradually returns to its initial flat state without compositional change through the evaporation of the ethanol under ambient conditions (Figure S5, Supporting Information). This curling and flattening cycle is fully repeatable for 5 times (**Figure 4**a,b). During the sixth switching cycle, the curl degree drops to ≈80.4° (Figure 4b and Figure S6a, Supporting Information) and the average storage modulus of the film reduces from ≈2.2×10^4 Pa to ≈1.1×10^3 Pa (**Figure 5**) due to the accumulated physical damages (Figure S6b, Supporting Information). However, the cracks in the BPEI/PAA portion of the heterostructure can be fully healed in 15 min simply by exposure to water (Figure S7, Supporting Information). The film storage modulus and loss modulus in frequency insensitive region,

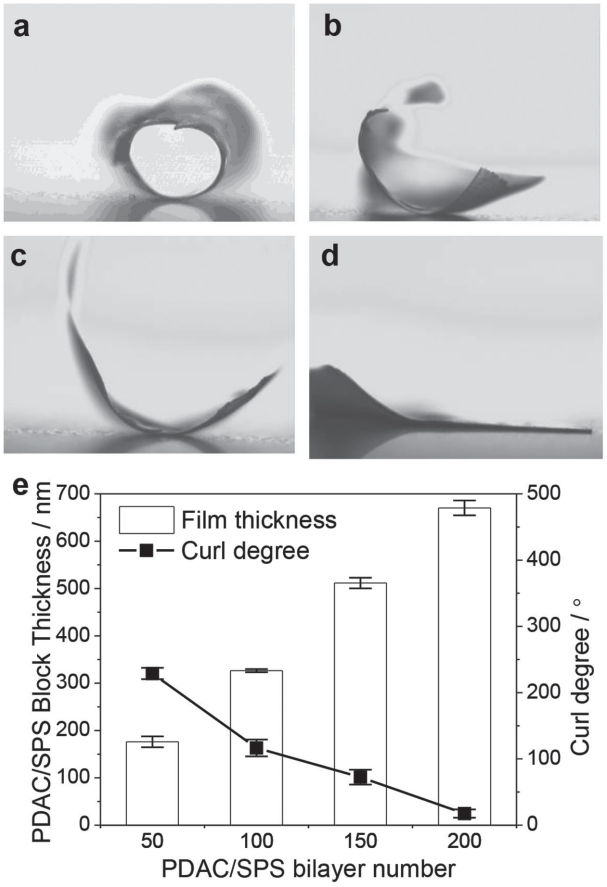

Figure 3. a) Photographs of the free-standing $(BPEI/PAA)_{50}/(PDAC/SPS)_{50}$ film, b) the $(BPEI/PAA)_{50}/(PDAC/SPS)_{100}$ film, c) the $(BPEI/PAA)_{50}/(PDAC/SPS)_{150}$ film, and d) the $(BPEI/PAA)_{50}/(PDAC/SPS)_{200}$ film treated by pure ethanol. e) The PDAC/SPS multilayer thickness and the curl degrees of the resulting $(BPEI/PAA)_{50}/(PDAC/SPS)_n$ films treated by pure ethanol.

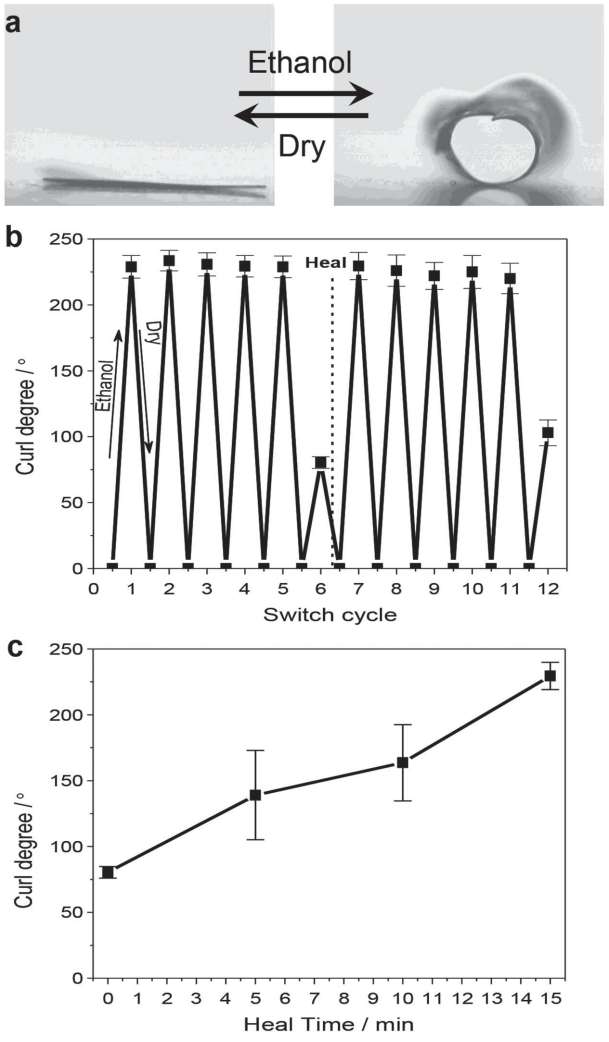

Figure 4. a) Photographs and b) curl degree of the free-standing $(BPEI/PAA)_{50}/(PDAC/SPS)_{50}$ film in dry state and dipped by ethanol. The movie of the reversible curling process is also available in the Supporting Information. c) The curl degree of the damaged $(BPEI/PAA)_{50}/(PDAC/SPS)_{50}$ film after self-healing for determined time.

respectively, recover to 2.4×10^4 Pa and »1.0×10^4 Pa (Figure 5), which are, respectively, ≈109.0% and 103.0% of the initial values. The value returning to slightly higher than initial is either a consequence of error within the measurement itself, or perhaps due to a lack of complete removal of the ethanol from the system. It has been shown that exposure to ethanol stiffens BPEI/PAA films.[23] Meanwhile, $G'(\omega)$ as well as $G''(\omega)$ is, as before, no longer sensitive to angular frequency (Figure 5 and Figure S8, Supporting Information), indicating recovery of the dynamic bonds within the film. This complete self-healing of the film is faster than when the film is attached to a rigid substrate.[41] Upon water treatment, the BPEI/PAA multilayer swells and becomes liquid-like behavior (Figure S9, Supporting Information), which allows it to flow and fill the gaps caused by the damage. This is possible because of the rheological properties of the hydrated film, which is such because of the solubility of the individual polyelectrolytes and also because the polyelectrolyte chains are only partially charged.[40] This partial charge of the polymer backbones means that the film itself is not highly crosslinked and allows for more mobility of the constituent polyelectrolytes and complexes. The average curl degree of the film terminated after healing for 5 min by vacuum drying is still ≈139.0°, but it increases to ≈163.6° after healing for 10 min, and it reaches ≈229.5° after 15 min of healing (Figure 4c), which is comparable to the original value. Incomplete recovery of curl degree is found if the healing time is below 15 min, as some random cracks remain (Figure S7, Supporting Information). The fully healed film actuates stably for another 5 cycles (Figure 4b).

The $(BPEI/PAA)_{50}$ film also becomes highly sticky upon wetting with water,[23] enabling the pasting of $(BPEI/PAA)_{50}$ films onto arbitrary substrates to form a functional asymmetrical structures for ethanol responsive actuations. After pasting a $(BPEI/PAA)_{50}$ film to the following substrates: paper, porous cellulose nitrate membrane, polyethersulfone (PES) membrane, and aluminum foil, these substrates were all able to curl towards the BPEI/PAA side upon ethanol treatment (curl degree 20.5°–220.5°, **Figure 6** and Figure S10, Supporting Information). The magnitude of the curling for BPEI/PAA pasted to

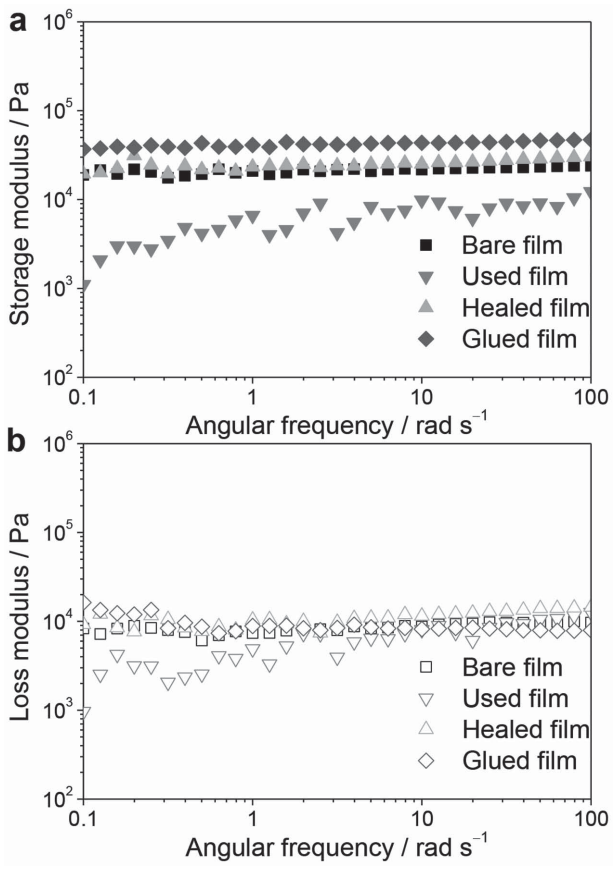

Figure 5. Angular frequency sweep plots of the bare $(BPEI/PAA)_{50}/(PDAC/SPS)_{50}$ film, the used $(BPEI/PAA)_{50}/(PDAC/SPS)_{50}$ film after repeated six curls, the self-healed $(BPEI/PAA)_{50}/(PDAC/SPS)_{50}$ film, and the film obtained by gluing two $(BPEI/PAA)_{50}/(PDAC/SPS)_{50}$ pieces by water treatment. a) Storage moduli; b) loss moduli.

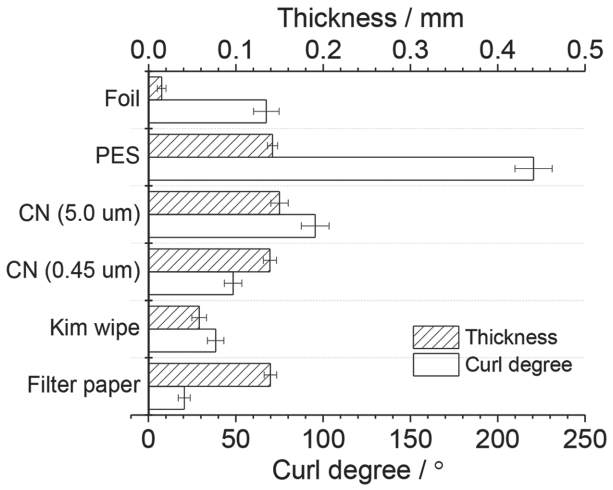

Figure 6. Initial substrate thickness and curl degrees of $(BPEI/PAA)_{50}$ pasted substrates upon ethanol treatment. Filter paper, kim wipe, porous cellulose nitrate membranes (CN, respective pore sizes 0.45 and 5.0 μm), porous PES membrane (pore size 0.45 μm), and aluminum foil were applied as substrates here.

paper is much greater than that of BPEI/PAA directly assembled onto paper (≈59°, Figure S11, Supporting Information), made by alternatively dipping paper in PE solutions. Paper's cellulose network is quite porous[44,45] and directly dipping paper into aqueous PE solutions allows them to diffuse into these pores. This prevents the formation of the distinct heterostructure required for large-scale actuation. With the paste-to-curl strategy, a freestanding BPEI/PAA multilayer is pasted to paper after assembly, which limits PE diffusion into the substrates' pores and allows for a distinct heterostructure to be formed. For the pasted actuator structures, a flexible substrate is favorable for creating high curl degree upon ethanol treatment, and substrates such as paper and porous cellulose nitrate membrane curl more significantly than aluminum foil which has a limited curl degree (67.4°). Among these various composite structures, $(BPEI/PAA)_{50}$ pasted onto PES membrane achieved the highest curl degree (220.5°), close to that of the $(PDAC/SPS)_{50}/(BPEI/PAA)_{50}$ film. The negatively charged ketone groups in PES are able to ionically bind with BPEI making a good interface between the PEM and the membrane. Video S2, Supporting Information, shows how quick the response is for a bilayer structure composed of the polyelectrolyte material adhered to a piece of PES and dipped into ethanol. **Figure 7**a shows a type of origami made with our composite actuator. A piece of PES membrane with has $(BPEI/PAA)_{50}$ films pasted on one side only at either end of the PES membrane and on the opposite side only in the middle, such that the composite regions did not overlap. The dry composite structure is flat, but it immediately curls into a shape similar to an omega (Ω) upon contact with

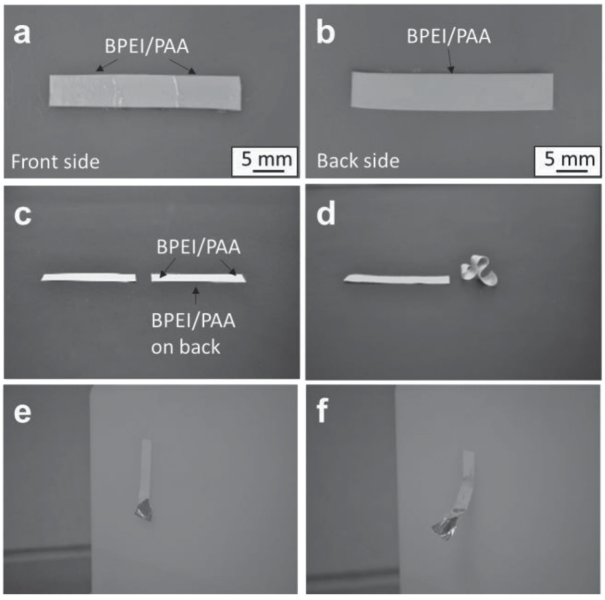

Figure 7. Photographs of the a) front side and b) back side of the $(BPEI/PAA)_{50}$ pasted PES. Photographs of the samples c) before and d) after wetting with ethanol. Left is a bare PES membrane and right is $(BPEI/PAA)_{50}$ pasted PES membrane. The $(BPEI/PAA)_{50}$ pasted PES is placed front side up, and ethanol was stained by 0.5 mg mL^{-1} methylene blue to envision the fully wetted state. A $(BPEI/PAA)_{50}$ pasted PES with a ≈50 mg aluminum sheet e) before and f) after wetting with ethanol. The sample is stuck on a vertical plastic wall, and only front side of the sample was pasted with a $(BPEI/PAA)_{50}$ film.

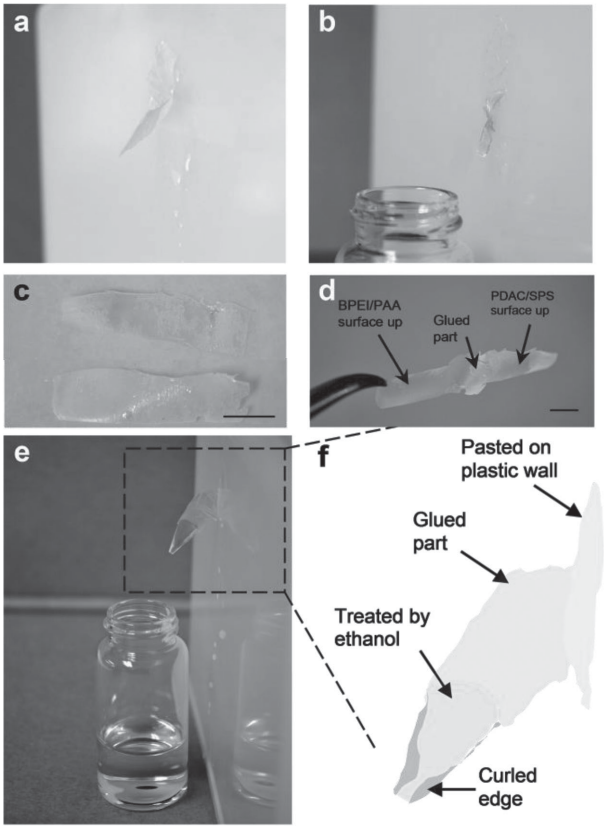

Figure 8. Photographs of $(BPEI/PAA)_{50}/(PDAC/SPS)_{50}$ film stuck on a vertical plastic wall a) before and b) after ethanol treatment, c) two bare $(BPEI/PAA)_{50}/(PDAC/SPS)_{50}$ pieces, and d) a composite film glued by wetting the two film pieces with DI water. The left part is BPEI/PAA side up, the right part is PDAC/SPS side up, and the center part is the glued portion in the composite film. Scale bars: 5 mm. e) Glued composite film pasted on a plastic wall. The right part adheres to water wetted plastic surface, and the left part curls by ethanol treatment. The vial with pure ethanol is placed to show that the plastic wall is vertically aligned. f) Schematic illustration of the adhered film in (e).

100% ethanol (Figure 7d). The center part curls down and the two ends curl up, while the ethanol treated bare PES membrane remains unchanged. Ethanol was stained by methylene blue prior to use for clear observation, and the porosity of the PES membrane allows for all BPEI/PAA portions to be evenly and concurrently exposed to the ethanol. Therefore, the curl direction depends on the position along the PES membrane that the BPEI/PAA film was pasted, and speed of actuation is much faster than other reports,[46] such as hydrated polymers (90° over 1 h),[34] micropatterned polymeric origami trilayers under UV light exposure (6° in 10 min),[47] blue light irradiated folding of hydrogel (stabilize in 3–4 min),[48] patterned carbon nanotube hydrogel composites in heated water (90° in 35–256 s).[49]

The adhesive nature of the $(BPEI/PAA)_{50}$ film once wet with water allows it to adhere the PES membrane to a plastic vertical wall (Figure 7e and Figure S12, Supporting Information). Onto the tip of the PES membrane surface, another piece of $(BPEI/PAA)_{50}$ film was used to attach a vial cap (≈500 mg), an aluminum ball (≈200 mg), or an aluminum sheet (≈50 mg) (Figure 7e and Figure S12, Supporting Information). The point of adhesion (≈0.25 cm^2) can support at least 600 mg weight regardless of the surface hydrophilicity and roughness of the materials being held up. Upon ethanol treatment, the $(BPEI/PAA)_{50}$ pasted on the front surface actuates and lifts up the small object. The weight that can be lifted is several hundred mg; for example the vial cap is too heavy for appreciable motion to be observed. However, even while supporting the heavier object, the system remains stable upon exposure to ethanol.

After soaking a free-standing $(BPEI/PAA)_{50}/(PDAC/SPS)_{50}$ heterostructure in DI water, its loss modulus increases by 1 order of magnitude and the relaxation time decreases from ≈90.9 to ≈3.5 s (Figure S9, Supporting Information), indicating an increase of mobility within the PEM structure. This also enhances the film's stickiness. The wet BPEI/PAA surface readily adheres to hydrophilic substrates (e.g., glass slides, silicon wafers, and aluminum foils), hydrophobic polystyrene plate, and even another $(BPEI/PAA)_{50}/(PDAC/SPS)_{50}$ piece (**Figure 8**). The film can be detached from hydrophobic surfaces without damage after drying because of the relatively weak surface interaction. This "sticky" quality is not seen for the SPS/PDAC film, at least in part because of the high density of ionic crosslinks in those films. When swollen in water, BPEI and PAA interactions in the film are weakened and chain motion is facilitated, which allows flexible PE chains to rearrange and increase effective contact area with the adjacent surface. With the evaporation of water, the water surface tension pushes the film tightly to the substrate, promoting mutual interaction like electrostatics to generate strong adhesion.[50]

By partially contacting two $(BPEI/PAA)_{50}/(PDAC/SPS)_{50}$ pieces face-to-face through BPEI/PAA side, they become well cross-linked as demonstrated by parallel $G'(\omega)$ and $G''(\omega)$ insensitive to angular frequency (Figure 5), forming an intact free-standing film with BPEI/PAA facing outward and up on half the structure and outward and down on the other half of the structure (Figure 8d). There is also an overlapping region in the center where the two pieces of PEM heterostructure were glued together. One of these BPEI/PAA faces was firmly stuck on a vertical plastic wall, and is able to suspend ≈157.7 mg of mass (corresponding to the weight of the PEM heterostructure) in the air with a contact area of ≈0.25 cm^2. The other BPEI/PAA surface can be seen to curl upon contact with ethanol (Figure 8). The curl degree decreases towards the center of the heterostructure where the two pieces were glued together as the region of overlap does not have the requisite asymmetric structure for actuation.

3. Conclusion

Presented here is the use of BPEI/PAA polyelectrolyte multilayers as a self-healing, wet adhesive actuating material. The actuating response is the result of fabricating an asymmetric heterostructure from both a nonresponsive component and the BPEI/PAA film which alone contracts upon exposure to alcohol. This contraction is due to a dehydration of the film occurring upon exposure to organic solvent. The removal of water closely bound to the PE chains results in a strengthening of the interactions between polymer backbones within the film and therefore a contraction of the film. The curl degree can be

as high as ≈228.9° by controlling the percentage of ethanol in the solution applied to the film and the thickness and modulus of the unresponsive component. The curled film spontaneously returns to its initial flat state with the evaporation of the ethanol under ambient conditions, and water initiated quick self-healing greatly extends the number of actuation cycles possible. Moreover, the adhesive quality of the BPEI/PAA film allows it to be adhered to a range of other materials, which can be potentially used for combination with hydrophobic functional surfaces and applications in biological environments. The current study on self-healable adhesive for controlled fast actuations opens a facile pathway for the development and applications of robust smart advanced materials.

4. Experimental Section

Materials: BPEI (M_w = 25 000), PDAC (average M_w 100 000–200 000, 20 wt% in H_2O), SPS (average M_w ≈70 000), ethanol, sodium hydroxide, hydrochloric acid, sulfuric acid, and hydrogen peroxide were purchased from Sigma-Aldrich. PAA (M_w = 50 000, 25 wt% solution) was bought from Polysciences. Filter paper (qualitative, size 12.5 cm), cellulose nitrate membrane filters (pore size 0.45 µm, ∅47 mm; pore size 5.0 µm, ∅47 mm), and PES membrane filter (pore size 0.45 µm, ∅47 mm) were purchased from VWR, Sterlitech, and Whatman, respectively. The DI water used in all the related experiments was purified by applying a Milli-Q DQ-3 system (Millipore, Bedford, MA, USA) with resistivity of 18.2 MΩ cm. All reagents were used as received without further purification. BPEI solution, 80×10^{-3} M with respect to the amine group of BPEI in DI water, stirred overnight and pH adjusted to 9.5 by adding 0.1 M hydrochloride solution; PAA solution, 60×10^{-3} M with respect to the carboxyl group of PAA in DI water, stirred overnight and pH adjusted to 4.5 by adding 0.1 M sodium hydroxide solution; PDAC solution, 20×10^{-3} M with respect to the amine group of PDAC in DI water; SPS solution, 20×10^{-3} M with respective to the sulfonate group of SPS in DI water. All the PE solutions were filtered prior to use. Piranha solution was freshly prepared by mixing 98% sulfuric acid with 30% hydrogen peroxide with a volume ratio of v/v = 7/3 prior to use.

Materials Fabrications: PEMs were assembled by LbL technique as reported previously (Scheme 1a).[23,26,41] Plastic substrates were first cleaned by successively rinsing with excess DI water and ethanol, and they were dried by nitrogen flow prior to use. PEMs were assembled sequentially at room temperature by applying a StratoSequence VI dipper (NanoStrata Inc., USA). Typically, the cleaned plastic substrates were first immersed in BPEI solution for 10 min, and then washed by three separate DI water rinse baths of 1 min each. Subsequently, these substrates were exposed to the PAA solution for 10 min and similarly washed with DI water. Thus, a thin BPEI/PAA multilayer was formed on the plastic substrate surface. By repeating the BPEI/PAA deposition cycle for 50 times, 50 BPEI/PAA bilayers were deposited on the plastic substrate. Then, PDAC and SPS were alternatively deposited through the identical PE exposure and rinsing procedure for 50 times, attaining a $(BPEI/PSS)_{50}/(PDAC/SPS)_{50}$ film coating on the plastic substrate. The resultant PEM films were dried at room temperature (≈25 °C) and atmospheric relative humidity (≈70%) for 24 h and peeled off from the plastic substrate for characterizations. Paper/$(PDAC/SPS)_{50}/(BPEI/PSS)_{50}$ was prepared through identical LbL process with quantitative filter paper (2 × 6 cm) as the substrate. The $(BPEI/PSS)_{50}/(PDAC/SPS)_{50}$ film was pasted to guest substrates through wetting the selected substrate surface with DI water and keeping the film in touch with substrate by facing the BPEI/PAA side to the substrate surface for 15 min. Similarly, gluing the two PEM film pieces was achieved by a facile water treatment. A film piece was placed on a plastic substrate facing BPEI/PAA side up, and then a second film piece was partially overlapped onto the first piece. The BPEI/PAA side of the second film piece was faced down to ensure the BPEI/PAA surfaces were in contact with each other. The overlapped part was wetted with DI water drops and dried under ambient condition. For paste-to-curl, $(BPEI/PAA)_{50}$ film was first deposited onto a polystyrene piece through above mentioned LbL process. The dry $(BPEI/PAA)_{50}$ film was peeled off from the polystyrene piece, and it was placed onto a selected substrate wetted with DI water. After drying in air, a free-standing sheet possessing directed curl behavior is formed. The thickness of the employed substrate was measured by a screw micrometer.

Characterizations: The average thickness of the dry film samples was calculated from the data acquired from five different positions of the film by employing a P-6 stylus profilometer (KLA Tencor Instruments, Milpitas, CA, USA). FTIR spectra were obtained by an Alpha-P FTIR spectrometer (Bruker Optics, Billerica, MA, USA) with ATR mode. The samples were analyzed immediately after vacuum drying overnight, and all measurements were carried out at room temperature (≈25 °C) with the atmospheric RH (≈70%). A 10 × 10 µm micrograph of the film surface morphology was obtained by using an atomic force microscope (Dimension ICON, Veeco) in tapping mode at 0.6 Hz using PPP-NCC-50 tips (Nanosensors). To examine the PEM film thickness change in ethanol-water mixture, $(BPEI/PAA)_6$ film and $(PDAC/SPS)_{50}$ film were, respectively, assembled on a piranha solution treated silicon wafer[26,41] and the resultant sample was tested in situ by a variable angle spectroscopic ellipsometer (VASE, M-2000 UV–visible–NIR [240–1700 nm] J. A. Woollam Co., Inc., Lincoln, NE, USA) equipped with a temperature controlled liquid cell (Scheme 1). The cell geometry dictated the angle of incidence to be 75°, and a limited wavelength range from 300 to 1150 nm was applied for the recursive fits due to the absorption of solvents in the ultraviolet and near-infrared light region. Standard window correction protocols with a silicon wafer with thermal oxide (25.0 nm) as the reference were used before each measurement.[51] The ellipsometry data were fitted by applying a four-layer model consisting of a silicon substrate layer, a fixed 1.0 nm Si–SiO_2 interface layer, a 0.8 nm thermal oxide layer, and a Cauchy layer (with thickness, A and B free fit parameters) in Complete EASE (J. A. Woollam, Co., Inc., Lincoln, NE, USA).[52] All in situ measurements were started at a fixed temperature of 25 °C. The PEM film was first measured in the dry state. After 1 min, selected solution was carefully charged to the cell by using a syringe to avoid possible air bubbles, and ambient index for the related solution model was meanwhile applied to fit the ellipsometric data. The determined refractive indices at 632 nm for water and ethanol are 1.333 and 1.478, respectively. The PEM sample was equilibrated in selected solution for 15 min in each case. Oscillatory shear measurements were carried out on a strain-controlled Advanced Rheometric Expansion System G2 rheometer (TA Instruments, USA) equipped with an 8 mm parallel plate and a bath trap at a gap of ≈0.030 mm at 25 °C. The linear response of the PEM was tested by a strain sweep from 0.05% to 100% at frequencies of 0.1, 1.0, 10.0, and 100.0 rad s^{-1}. Angular frequency sweeps from 0.1 to 100.0 rad s^{-1} were obtained at strain amplitude of 0.50%, which locates in the stable strain% region. The curl degree was evaluated based on the standard measurement of sheet curl degree.[42] Each free-standing PEM film was cut into 2 × 5 mm, and the specimen was placed on the desktop in front of a camera. At the ambient condition, selected solution (1.5 µL) was dropped onto the BPEI/PAA side of the film sample, upon which the sample curled up. After stabilization, the photograph of the solution treated specimen was taken to calculate the tangent line angle of the specimen curled end (Scheme S1a, Supporting Information). The average value of the left angle (A1) and right angle (A2) is determined as the curl degree. Five curl degree angle measurements of each sample were collected for the mean curl degree. Self-healing of the PEM film was proceeded by placing the damaged film on a clean plastic substrate, wetting the film with DI water (10 µL) and left at ambient condition for a determined period. The self-healing was stopped by removing the excess water and vacuum dried overnight. To test the reversibility of the curling process, the dry flat PEM film was first curled by wetting with pure ethanol (1.5 µL), and the curled film gradually flattened with the evaporation of ethanol component in 15 min at room temperature.

Supporting Information

Supporting Information is available from the Wiley Online Library or from the author.

Acknowledgements

This work was supported by National Science Foundation Grant No. DMR 1425187 and ARO STIR Contract No. W911NF-14–1–0587.

Received: March 17, 2015
Revised: April 21, 2015
Published online: May 15, 2015

[1] M. A. Cohen Stuart, W. T. S. Huck, J. Genzer, M. Müller, C. Ober, M. Stamm, G. B. Sukhorukov, I. Szleifer, V. V. Tsukruk, M. Urban, F. Winnik, S. Zauscher, I. Luzinov, S. Minko, *Nat. Mater.* **2010**, *9*, 101.
[2] E. M. White, J. Yatvin, J. B. Grubbs, J. A. Bilbrey, J. Locklin, *J. Polym. Sci., Part B: Polym. Phys.* **2013**, *51*, 1084.
[3] R. Yoshida, K. Uchida, Y. Kaneko, K. Sakai, A. Kikuchi, Y. Sakurai, T. Okano, *Nature* **1995**, *374*, 240.
[4] Z. Hu, X. Zhang, Y. Li, *Science* **1995**, *269*, 525.
[5] J. Kopeček, *Nature* **2002**, *417*, 388.
[6] E. Smela, *Adv. Mater.* **2003**, *15*, 481.
[7] Q. Zhao, J. W. Dunlop, X. Qiu, F. Huang, Z. Zhang, J. Heyda, J. Dzubiella, M. Antonietti, J. Yuan, *Nat. Commun.* **2014**, *5*, 4293.
[8] J. Kim, J. H. Jeon, H. J. Kim, H. Lim, I. K. Oh, *ACS Nano* **2014**, *8*, 2986.
[9] A. Reisch, E. Roger, T. Phoeung, C. Antheaume, C. Orthlieb, F. Boulmedais, P. Lavalle, J. B. Schlenoff, B. Frisch, P. Schaaf, *Adv. Mater.* **2014**, *26*, 2547.
[10] S. Michel, B. T. T. Chu, S. Grimm, F. A. Nüesch, A. Borgschulte, D. M. Opris, *J. Mater. Chem.* **2012**, *22*, 20736.
[11] S. Hunt, T. G. McKay, I. A. Anderson, *Appl. Phys. Lett.* **2014**, *104*, 113701.
[12] Y. Li, L. Li, J. Sun, *Angew. Chem. Int. Ed.* **2010**, *49*, 6129.
[13] X. Wang, F. Liu, X. Zheng, J. Sun, *Angew. Chem. Int. Ed.* **2011**, *50*, 11378.
[14] A. B. South, L. A. Lyon, *Angew. Chem. Int. Ed.* **2010**, *49*, 767.
[15] Y. Lu, X. Chen, W. Hu, N. Lu, J. Sun, J. Shen, *Langmuir* **2007**, *23*, 3254.
[16] Y. Li, S. Chen, M. Wu, J. Sun, *Adv. Mater.* **2012**, *24*, 4578.
[17] M. M. Caruso, D. A. Davis, Q. Shen, S. A. Odom, N. R. Sottos, S. R. White, J. S. Moore, *Chem. Rev.* **2009**, *109*, 5755.
[18] A. P. Esser-Kahn, N. R. Sottos, S. R. White, J. S. Moore, *J. Am. Chem. Soc.* **2010**, *132*, 10266.
[19] B. J. Blaiszik, S. L. B. Kramer, S. C. Olugebefola, J. S. Moore, N. R. Sottos, S. R. White, *Annu. Rev. Mater. Res.* **2010**, *40*, 179.
[20] J.-H. Park, P. V. Braun, *Adv. Mater.* **2010**, *22*, 496.
[21] S. H. Cho, S. R. White, P. V. Braun, *Adv. Mater.* **2009**, *21*, 645.
[22] C. J. Hansen, W. Wu, K. S. Toohey, N. R. Sottos, S. R. White, J. A. Lewis, *Adv. Mater.* **2009**, *21*, 4143.
[23] Y. Gu, X. Huang, C. G. Wiener, B. D. Vogt, N. S. Zacharia, *ACS Appl. Mater. Interfaces* **2015**, *7*, 1848.
[24] X. Gong, C. Gao, *Phys. Chem. Chem. Phys.* **2009**, *11*, 11577.
[25] S. Ahn, R. M. Kasi, S.-C. Kim, N. Sharma, Y. X. Zhou, *Soft Matter* **2008**, *4*, 1151.
[26] X. Huang, J. D. Chrisman, N. S. Zacharia, *ACS Macro Lett.* **2013**, *2*, 826.
[27] K. Glinel, C. Déjugnat, M. Prevot, B. Schöler, M. Schönhoff, R. V. Klitzing, *Colloids Surf., A* **2007**, *303*, 3.
[28] T. Kimura, S. Takahashi, S. Akiyama, T. Uzawa, K. Ishimori, I. Morishima, *J. Am. Chem. Soc.* **2002**, *124*, 11596.
[29] R. Zahn, J. Vörös, T. Zambelli, *Langmuir* **2014**, *30*, 12057.
[30] D. J. Schmidt, Y. Min, P. T. Hammond, *Soft Matter* **2011**, *7*, 6637.
[31] G. Ibarz, L. Dähne, E. Donath, H. Möhwald, *Chem. Mater.* **2002**, *14*, 4059.
[32] L. Shen, J. Fu, K. Fu, C. Picart, J. Ji, *Langmuir* **2010**, *26*, 16634.
[33] Y. Ma, Y. Zhang, B. Wu, W. Sun, Z. Li, J. Sun, *Angew. Chem. Int. Ed.* **2011**, *50*, 6254.
[34] B. P. Lee, S. Konst, *Adv. Mater.* **2014**, *26*, 3415.
[35] J. Choi, M. F. Rubner, *Macromolecules* **2005**, *38*, 116.
[36] I. A. Mudunkotuwa, A. A. Minshid, V. H. Grassian, *Analyst* **2014**, *139*, 870.
[37] D. Kim, P. Tzeng, K. J. Barnett, Y.-H. Yang, B. A. Wilhite, J. C. Grunlan, *Adv. Mater.* **2014**, *26*, 746.
[38] B. Torger, M. Müller, *Spectrochim. Acta, Part A* **2013**, *104*, 546.
[39] L. Zhang, L. R. Kucera, S. Ummadisetty, J. R. Nykaza, Y. A. Elabd, R. F. Storey, K. A. Cavicchi, R. A. Weiss, *Macromolecules* **2014**, *47*, 4387.
[40] C. Picart, J. Mutterer, L. Richert, Y. Luo, G. D. Prestwich, P. Schaaf, J.-C. Voegel, P. Lavalle, *Proc. Natl. Acad. Sci. U.S.A.* **2002**, *99*, 12531.
[41] X. Huang, M. J. Bolen, N. S. Zacharia, *Phys. Chem. Chem. Phys.* **2014**, *16*, 10267.
[42] F. T. Carson, V. Worthington, *J. Res. Natl. Bur. Stand.* **1943**, *30*, 113.
[43] M. Matsusaki, H. Ajiro, T. Kida, T. Serizawa, M. Akashi, *Adv. Mater.* **2012**, *24*, 454.
[44] Y. Gu, T. Niu, J. Huang, *J. Mater. Chem.* **2010**, *20*, 10217.
[45] Y. Gu, J. Huang, *J. Mater. Chem.* **2009**, *19*, 3764.
[46] D. Chen, J. Yoon, D. Chandra, A. J. Crosby, R. C. Hayward, *J. Polym. Sci., Part B: Polym. Phys.* **2014**, *52*, 1441.
[47] J.-H. Na, A. A. Evans, J. Bae, M. C. Chiappelli, C. D. Santangelo, R. J. Lang, T. C. Hull, R. C. Hayward, *Adv. Mater.* **2015**, *27*, 79.
[48] J. Yoon, P. Bian, J. Kim, T. J. McCarthy, R. C. Hayward, *Angew. Chem. Int. Ed.* **2012**, *51*, 7146.
[49] X. Zhang, C. L. Pint, M. H. Lee, B. E. Schubert, A. Jamshidi, K. Takei, H. Ko, A. Gillies, R. Bardhan, J. J. Urban, M. Wu, R. Fearing, A. Javey, *Nano Lett.* **2011**, *11*, 3239.
[50] K. E. Bremmell, P. J. Scales, *Colloids Surf. A* **2004**, *247*, 19.
[51] Z. Qiang, J. Xue, K. A. Cavicchi, B. D. Vogt, *Langmuir* **2013**, *29*, 3428.
[52] C. Herzinger, B. Johs, W. A. McGahan, J. A. Woollam, W. Paulson, *J. Appl. Phys.* **1998**, *83*, 3323.